

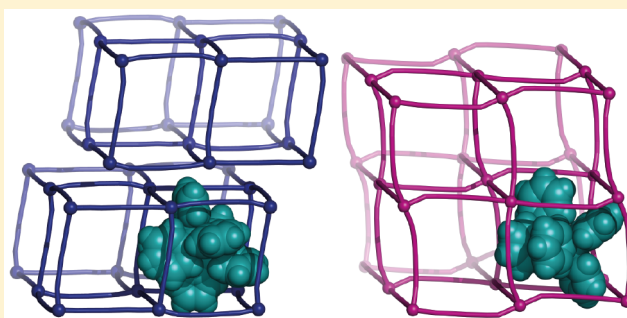
Dicyanometallates as Model Extended Frameworks

Joshua A. Hill, Amber L. Thompson, and Andrew L. Goodwin*

Inorganic Chemistry Laboratory, Department of Chemistry, University of Oxford, South Parks Road, Oxford OX1 3QR, U.K.

S Supporting Information

ABSTRACT: We report the structures of eight new dicyanometallate frameworks containing molecular extra-framework cations. These systems include a number of hybrid inorganic–organic analogues of conventional ceramics, such as Ruddlesden–Popper phases and perovskites. The structure types adopted are rationalized in the broader context of all known dicyanometallate framework structures. We show that the structural diversity of this family can be understood in terms of (i) the charge and coordination preferences of the particular metal cation acting as framework node, and (ii) the size, shape, and extent of incorporation of extra-framework cations. In this way, we suggest that dicyanometallates form a particularly attractive model family of extended frameworks in which to explore the interplay between molecular degrees of freedom, framework topology, and supramolecular interactions.



INTRODUCTION

Arguably one of the most important conceptual breakthroughs in modern structural chemistry was Robson's geometric interpretation of the structures of coordination polymers as connected nets of nodes and linkers.¹ The language of reticular chemistry that developed from that point has enabled the informed design of an extraordinarily large family of framework materials and coordination polymers, notably including metal–organic frameworks (MOFs)² and covalent organic frameworks (COFs).^{3,4} The basic design approach as it is currently used reflects the realization that specific combinations of node and linker geometries can usually lead to only a finite number of different possible structures;⁵ hence, control over the former (e.g., the choice of transition-metal elements or clusters with specific coordination geometry preferences and linkers with characteristic binding modes) enables control over the latter.⁶

The abstraction of linker molecules to rodlike connections carries with it the implication that linker shape and chemistry bear little influence on the resulting framework structure. Certainly this is sometimes true,^{7,8} but for many coordination polymers the packing motifs and stereochemical preferences of the organic linkers often play a defining role in directing structure. This may be as simple as linker functionalization preventing network interpenetration but the effects can also be altogether more drastic.⁹ For example, if the terephthalate linker connecting chains of corner-sharing $\text{AlO}_4(\text{OH})_2$ octahedra in the porous “breathing” MIL-53 (ref 10) is swapped for the longer and slightly bent 4,4'-azobenzene dicarboxylate then the nonporous layered MIL-129 forms instead, where the ligands now adopt a π – π stacking motif.¹¹

It is in this context that we have developed a particular interest in coordination polymers assembled using the dicyanometallate linker $[\text{NC}-\text{M}-\text{CN}]^-$ ($\text{M} = \text{Cu}^{\text{I}}$, Ag^{I} , Au^{I}).

The preferred coordination mode of this linker is linear, and so it combines the nanometre scale of the organic linkers used to build MOFs with the geometric flexibility of an atomically thin linker. In many ways, dicyanometallates can be considered the natural extension of oxide frameworks (e.g., perovskites) and cyanide frameworks (e.g., Prussian Blues) [Figure 1].

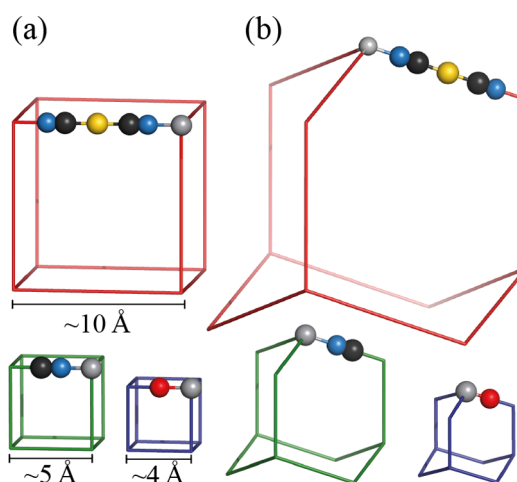


Figure 1. Increasing scale of oxide (blue), cyanide (green), and dicyanometallate (red) architectures illustrated with the perovskite (a) and cristobalite (b) structures. Increasing the length of the linker dramatically increases the available volume for interpenetration, extra-framework cations, and/or neutral guests. Node metal (gray), oxygen (red), nitrogen (blue), carbon (black), and linker metal (yellow).

Received: December 24, 2015

Published: April 8, 2016

Table 1. Summary of the Structurally Characterized Dicyanometallate Frameworks of General Formula $A_nB(L)X_m \cdot G$, Where L Is a Neutral Ligand Bound to the Node Metal Center (i.e., Not to the Linker Metal) and G Is a Non-coordinating Guest Molecule^a

B^IX Chains	Coordination number = 2	B^{II}X₂ Square grid	4	B^{II}X₂ Interpenetrating square grid	4	AB^{III}X₃ α-Po	6
Parallel AuCN ^{34,35} AgCN ^{35,39,40} CuCN ⁴⁴ Ni(L ¹)(H ₂ O)Ag(CN) ₂ ⁴⁷ Criss-cross low-T Cu(CN) ⁴⁴		Regular Cu(py) ₂ [Au(CN) ₂] ₂ ³⁶ Fe(3-Phpy) ₂ [Au(CN) ₂] ₂ ⁴¹ yellow-Fe(3-CNpy) ₂ [Au(CN) ₂] ₂ ⁴⁵ Fe(DEAS) ₂ [Au/Ag(CN) ₂] ₂ ⁴⁸ Cd(py) ₂ [Ag(CN) ₂] ₂ ⁴⁹ Fe(py) ₂ [Ag(CN) ₂] ₂ ⁵²		Inclined Cd(NH ₃) ₂ [Ag(CN) ₂] ₂ ³⁷ Cu(NH ₃) ₂ [Ag(CN) ₂] ₂ ⁴² Zn(NH ₃) ₂ [Au(CN) ₂] ₂ ¹⁴ Cd(py) ₂ [Ag(CN) ₂] ₂ ·C ₄ H ₅ N ⁴⁹ Cd(py) ₂ [Ag(CN) ₂] ₂ ·C ₆ H ₆ ⁴⁹ Mn(4-Mepy) ₂ [Ag(CN) ₂] ₂ ⁵³		KCo[Au(CN) ₂] ₃ ^{15,33} RbCd[Ag(CN) ₂] ₃ ³⁸ KNi[Au(CN) ₂] ₃ ⁴³ KMn[Ag(CN) ₂] ₃ ⁴⁶ KCd[Au/Ag(CN) ₂] ₃ ⁵⁰ KFe[Au/Ag(CN) ₂] ₃ ^{19,51}	
A_{0.5}B^IX_{1.5} (6,3) layers [Cu ₂ (2,2'-bpy) ₂ (CN)] _{0.5} Cu[Cu(CN) ₂] _{1.5} ⁵⁵	3	Cu(DMF)[Au(CN) ₂] ₂ ¹⁷ blue-Cu(DMSO) ₂ [Au(CN) ₂] ₂ ¹⁷ Zn(NIT4Py) ₂ [Au(CN) ₂] ₂ ⁵⁶ Pb(phen) ₂ [Au(CN) ₂] ₂ ⁵⁷ Fe(H ₂ O) ₂ [Ag(CN) ₂] ₂ ·(2,2'-bpe) ⁵⁹ ($\frac{1}{2}$, $\frac{1}{2}$) offset bilayers Co(DMF) ₂ [Au(CN) ₂] ₂ ⁶¹ Mn(3-Fpy) ₂ [Au(CN) ₂] ₂ ⁶² Mn(H ₂ O) ₂ [Au(CN) ₂] ₂ ⁵¹ Mn(3-Mepy) ₂ [Ag(CN) ₂] ₂ ⁵³ colourless-Fe(3-CNpy) ₂ [Au(CN) ₂] ₂ ·H ₂ O ⁴⁵ Fe(4-Mepy) ₂ [Au(CN) ₂] ₂ ⁶⁵ Fe(3-Clpy) ₂ [Au/Ag(CN) ₂] ₂ ^{66,67} Fe(3-Brpy) ₂ [Au/Ag(CN) ₂] ₂ ^{66,67} Fe(3-Ipy) ₂ [Au/Ag(CN) ₂] ₂ ^{66,67} Fe(3-Ipy) ₂ [Au(CN) ₂] ₂ · $\frac{1}{2}$ ·3-Ipy ⁶⁷ Fe(3-Fpy) ₂ [Au/Ag(CN) ₂] ₂ ^{66,67} Cd(3-Fpy) ₂ [Au(CN) ₂] ₂ ⁷⁴ Mn(bim)[Ag(CN) ₂] ₂ ·[(bim)AgCN] ₂ ·nH ₂ O ⁷⁶ Bridged (Hofmann) Zn(py ₂)[Au(CN) ₂] ₂ ⁷⁹ Co(py ₂)[Au(CN) ₂] ₂ ⁷⁹ Cd(4,4'-bpy)[Ag(CN) ₂] ₂ ⁸² Mn(4,4'-bpy)[Au(CN) ₂] ₂ ·2CHCl ₃ ⁸⁵ Cu(py ₂)[Au(CN) ₂] ₂ ⁸⁷ Fe(bpmp)[Au/Ag(CN) ₂] ₂ ·nDMF· $\frac{1}{2}$ ·EtOH·mH ₂ O ⁹⁰ Fe(py ₂)[Au(CN) ₂] ₂ ·(py ₂) ¹⁸		Interwoven Ca[Ag(CN) ₂] ₂ ·2H ₂ O ⁵⁴ Sr[Ag(CN) ₂] ₂ ·2H ₂ O ⁵⁴ Cd(4-Mepy) ₂ [Ag(CN) ₂] ₂ ·(4-Mepy) ⁵⁸ B^{II}X₂ Other Two layer herringbone Cd(hydeten)[Ag(CN) ₂] ₂ · $\frac{1}{2}$ ·H ₂ O ⁶³ Bifurcated chains Mn(NIT3Py) ₂ [Au(CN) ₂] ₂ ⁶⁴ Co(NIT3Py) ₂ [Au(CN) ₂] ₂ ⁶⁴ Zn(NIT3Py) ₂ [Au(CN) ₂] ₂ ⁶⁴ Bridged interwoven (6,3) (mok) δ-Zn[Au(CN) ₂] ₂ ¹⁴ lvt Mn(4-CNpy)(H ₂ O)[Ag(CN) ₂] ₂ ⁷¹ Binodal (pts) Mn(py-4-aldoxime)(H ₂ O)[Ag(CN) ₂] ₂ ⁷¹ A_{0.5}B^IX_{2.5} Layered Perovskite slabs [PPN] _{0.5} Cu[Au(CN) ₂] _{2.5} ·EtOH* [PPN] _{0.5} Cd[Ag(CN) ₂] _{2.5} (EtOH)* [PPN] _{0.5} Mn[Ag(CN) ₂] _{2.5} (EtOH)* A_{0.5}B^IX_{2.5} Other Bridged interwoven (6,3) (jah1) [Bu ₄ N] _{0.5} Cd[Ag(CN) ₂] _{2.5} *		AB^{III}X₃ Perovskite [PPN]Ni[Au(CN) ₂] ₃ ³² [PPN]Co[Au(CN) ₂] ₃ ³² [PPN]Cd[Au(CN) ₂] ₃ * [PPN]Mn[Au(CN) ₂] ₃ * [PPN]Cd[Ag(CN) ₂] ₃ ·3EtOH·xH ₂ O* AB^{III}X₃ Other Intersecting rectangular grids (bcs) [Bu ₄ N]Ni[Au(CN) ₂] ₃ ³² B^{III}X₃ α-Po Ag ₃ [Co(CN) ₆] ₆ ⁶⁸ Ag ₃ [Fe(CN) ₆] ₆ ⁶⁹ Au/Ag ₃ [In(CN) ₆] ₆ ⁵⁰ Ag ₃ [In(CN) ₆] ₆ ·xH ₂ O ⁵⁰ B^{III}X₃ acs La[Au/Ag(CN) ₂] ₃ (H ₂ O) ₃ ⁷⁷ La[Ag _{0.39} Au _{0.61} (CN)] ₃ (H ₂ O) ₃ ⁷⁷ La[Ag _{0.83} Au _{0.17} (CN)] ₃ (H ₂ O) ₃ ⁷⁷ Pr[Au/Ag(CN) ₂] ₃ (H ₂ O) ₃ ⁸⁰ Nd[Au/Ag(CN) ₂] ₃ (H ₂ O) ₃ ⁸³ Sm[Au(CN)] ₃ (H ₂ O) ₃ ⁸⁶ Eu[Au/Ag(CN) ₂] ₃ (H ₂ O) ₃ ^{88,89} Eu _{0.5} Tb _{0.5} [Au(CN)] ₃ (H ₂ O) ₃ ⁸⁹ Gd[Au(CN)] ₃ (H ₂ O) ₃ ⁹¹ Tb[Au(CN)] ₃ (H ₂ O) ₃ ^{92,93} Am[Au/Ag(CN) ₂] ₃ (H ₂ O) ₃ ⁸³ Cm[Au/Ag(CN) ₂] ₃ (H ₂ O) ₃ ⁸⁰	
AB^IX₂ Square grids Wavy KCu[Ag(CN) ₂] ₂ ⁶⁰ RbCu[Ag(CN) ₂] ₂ ⁶⁰ CsCu[Ag(CN) ₂] ₂ ⁶⁰ AB^IX₂ Diamondoid Distorted [NEt ₄][Ag[Ag(CN) ₂] ₂]* B^{II}X₂ Quartz α-Zn[Au(CN) ₂] ₂ ⁷⁰ Co[Au(CN) ₂] ₂ ⁷² α-Zn[Ag(CN) ₂] ₂ ·xAg(CN) ⁷³ Cd(2,2'-bpy)[Au(CN) ₂] ₂ ⁷⁵ Mn(2,2'-bpy)[Au(CN) ₂] ₂ ⁷⁸ B^{II}X₂ Niobium monoxide (nbo) Fe(3-CNpy) ₂ [Au/Ag(CN) ₂] ₂ · $\frac{2}{3}$ ·H ₂ O ^{45,81} Fe(TPT) _{2/3} [Au/Ag(CN) ₂] ₂ ⁸⁴ Fe(TPT) _{2/3} [Au/Ag(CN) ₂] ₂ ·2CH ₂ Cl ₂ ⁸⁴ Fe(TPT) _{2/3} [Ag(CN) ₂] ₂ ·MeOH ⁸⁴ B^{II}X₂ Cadmium sulfate (cads) Fe(pmd)(H ₂ O)[Au(CN) ₂] ₂ ·H ₂ O ⁹⁴ Fe(pmd)(H ₂ O)[Ag(CN) ₂] ₂ ·H ₂ O ⁹⁴ Fe(pmd)[Au(CN) ₂] ₂ ⁹⁴		B^{II}X₂ Cristoballite β-Zn[Au(CN) ₂] ₂ ¹⁴ γ-Zn[Au(CN) ₂] ₂ ¹⁴					

^aFormulae including Au/Ag indicate that both the pure gold- and silver-containing compounds are known. Newly synthesized compounds reported as part of our study are indicated by an asterisk. Abbreviations used: L¹ = N-(3-aminopropyl)-5-bromosalicylaldehyde; 2,2'-bpy = 2,2'-bipyridine; Et = C₂H₅; 3-CNpy = 3-cyanopyridine; TPT = 2,4,6-tris(priidyl)triazine; Me = CH₃; pmd = pyrimidine; py = pyridine; 3-Phpy = 3-phenylpyridine; DEAS = 4'-diethylaminostilbazole; DMF = N,N'-dimethylformamide; DMSO = dimethyl sulfoxide; NIT4Py = 2-(4'-pyridyl)-4,4,5,5-tetramethylimidazoline-1-oxyl-3-oxide; phen = 1,10-phenanthroline; 2,2'-bpe = 2,2'-bis(pyridyl)ethene; 3-Fpy = 3-fluoropyridine; 3-Mepy = 3-methylpyridine; 4-Mepy = 4-methylpyridine; 3-Clpy = 3-chloropyridine; 3-Brpy = 3-bromopyridine; 3-Ipy = 3-iodopyridine; bim = benzimidazole; pyz = pyrazine; 4,4'-bpy = 4,4'-bipyridine; bpmp = 1,4-bis(pyridin-4-ylmethyl)piperazine; hydeten = N-(2-hydroxyethyl)ethylenediamine; NIT3Py = 2-(3'-pyridyl)-4,4,5,5-tetramethylimidazoline-1-oxyl-3-oxide; PPN = bis(triphenylphosphine)iminium cation; Bu = n-C₄H₉.

Like their oxide and cyanide cousins, dicyanometallate frameworks exhibit a variety of important functional responses. Examples include colossal positive and negative thermal expansion in silver hexacyanocobaltate (\equiv Co^{III}[Ag^I(CN)₂]₃);¹² giant negative compressibility and guest-dependent luminescence in Zn[Au(CN)₂]₂;^{13,14} piezoelectric behavior in KCo[Au(CN)₂]₃;¹⁵ tunable room-temperature luminescence in La[Au_xAg_{1-x}(CN)₂]₃·3H₂O;¹⁶ vapochromism

in Cu[Au(CN)₂]₂;¹⁷ heat-, light-, and pressure-induced spin-crossover in Fe(py₂)[Ag(CN)₂]₂·pyz (pyz = pyrazine);¹⁸ and strain-free charge storage in K_xFe^{II/III}[Ag(CN)₂]₃.¹⁹ In each of these cases, the geometric flexibility of the dicyanometallate linker plays a key role and so there is good reason to expect similarly intriguing functional responses among as-yet-unrealised dicyanometallate frameworks. Yet, in this context of developing new functional dicyanometallates, what is con-

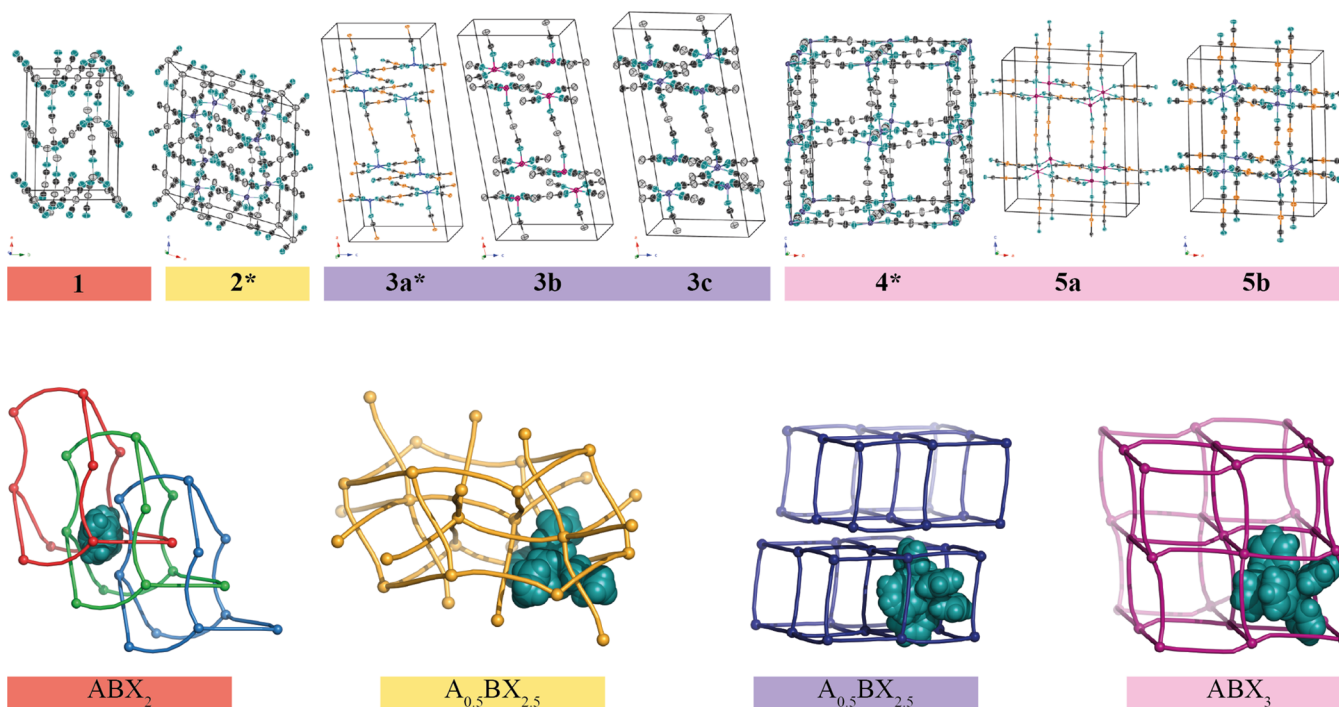


Figure 2. Representations of the crystal structures of the various new dicyanometallate frameworks reported in this study. The top panels show structures in thermal ellipsoid representation (probability = 50%, or 90% where indicated with an asterisk). Each image is represented at the same absolute scale; extra-framework cations and solvent molecules have been omitted for clarity. The bottom panels show schematic representations of the corresponding network topologies. In each case a single extra-framework cation is shown in space-filling representation to illustrate the relationship between cation shape and network topology. More detailed representations are given as SI.

spicuously absent is an overview of the structural chemistry of the family of the sort that has been so enabling in, e.g., oxide^{20,21} and cyanide^{22–24} framework chemistry.

Table 1 summarizes, to the best of our knowledge, the various dicyanometallate frameworks reported to date. For simplicity, we have focused on systems expressible in the form $A_mBX_n \cdot \{\text{guest}\}$. In this representation, A denotes an extra-framework cation (if present), B is the framework node cation, X is a dicyanometallate anion, and we allow for the presence of solvent or other neutral molecules within the structure. What is immediately clear is that the family is extremely diverse, and encompasses much of the compositional and topological complexity responsible for the rich structural chemistry of conventional ceramic frameworks. In addition, and as in the transition-metal formate “MOF perovskites”,^{25–27} there is the intriguing capacity to incorporate molecular cations as a means of balancing framework charge. There is strong current interest in these systems as a direct result of the recent discovery of unconventional semiconductor behavior in the $[\text{CH}_3\text{NH}_3]\text{PbI}_3$ family of solar cell materials.^{28–30} Ordering processes involving molecular cations can be fundamentally different from those involving spherically symmetric or dipolar cations, as in conventional oxide ceramics.³¹ The relationship between molecular geometry and host framework topology remains relatively unexplored—particularly in dicyanometallates.³² Likewise, the nanometre node separation in dicyanometallate frameworks potentially allows for the incorporation of molecular cations capable of complex supramolecular interactions.

Our paper has two principal objectives. The first aim is to report the structures of a number of new dicyanometallate frameworks which contain molecular cations. On the one hand,

these are of fundamental interest in terms of their structural chemistry, but on the other hand they may prove important by virtue of their conceptual relationship to other molecular analogues of conventional ceramics, including the semi-conducting lead iodide family. The second—and ultimately more important—aim of our study is to suggest an organization of the structures of known dicyanometallates that helps rationalize the structural diversity of this family. In doing so we begin to develop a set of design strategies that will ultimately allow rational control over framework structure in precisely the way envisaged by Robson’s original study.¹

RESULTS AND DISCUSSION

Structural Investigation of New Dicyanometallates.

Our starting point is to describe the various new dicyanometallates we have prepared. Motivated by the desire to introduce molecular extra-framework cations, our typical synthetic strategy was to combine a simple transition-metal salt with a specially prepared molecular salt of a given dicyanometallate anion. The latter acts as the source of molecular cation in the framework that ultimately forms. We report eight new compounds, which adopt a total of five structure types and correspond to the three fundamental compositions ABX_2 , $A_{0.5}BX_{2.5}$, and ABX_3 .

Diamondoid ABX_2 . The first system we describe was actually the fortuitous result of our attempts to prepare $[\text{NEt}_4][\text{Ag}(\text{CN})_2]$ as a dicyanometallate precursor for subsequent framework formation. The combination of $[\text{NEt}_4]\text{Cl}$ or $[\text{NEt}_4]\text{Br}$ with $\text{KAg}(\text{CN})_2$ yields the same dicyanometallate framework $[\text{NEt}_4][\text{Ag}^{\text{I}}[\text{Ag}(\text{CN})_2]_2]$ (1) in which silver(I) cations participate as both node and linker. The dual roles of silver(I) in this system are distinguishable by both coordination

Table 2. Crystallographic Details for the New Materials Reported in This Study

Compound	1	2	3a	3b
Empirical formula	Ag ₃ N ₅ C ₁₂ H ₂₀	Cd ₂ Ag ₅ N ₁₁ C ₂₆ H ₃₆	Cu ₂ Au ₅ P ₂ N ₁₁ C ₄₆ H ₃₀	Mn ₂ Ag ₅ P ₂ N ₁₁ C ₄₆ H ₃₀
Formula weight (g mol ^{−1})	557.92	1266.79	2002.83	1540.1
Crystal System	Orthorhombic	Monoclinic	Monoclinic	Monoclinic
Space Group	<i>Pnma</i> (No. 62)	<i>C2/c</i> (No. 15)	<i>C2/c</i> (No. 15)	<i>C2/c</i> (No. 15)
Z	4	4	4	4
Radiation (Å)	Cu K α , λ = 1.54180	Mo K α , λ = 0.71073	λ = 0.68890	Cu K α , λ = 1.54180
Crystal colour	Pale Yellow	Colourless	Green	Colourless
Crystal size (mm)	0.05 × 0.11 × 0.12	0.06 × 0.14 × 0.16	0.01 × 0.01 × 0.01	0.09 × 0.22 × 0.27
Temperature (K)	280.2(5)	150.0(5)	30.0(3)	300.00(3)
<i>a</i> (Å)	16.6101(3)	16.2798(2)	27.9505(6)	28.3700(3)
<i>b</i> (Å)	11.2973(2)	13.9248(2)	15.0898(4)	15.6843(2)
<i>c</i> (Å)	9.2725(2)	18.0439(2)	13.4803(3)	13.91760(10)
<i>V</i> (Å ³)	1739.98(6)	3930.35(9)	5647.5(2)	6105.94(11)
β (°)	—	106.0823(5)	96.629(2)	99.6092(10)
μ (mm ^{−1})	26.795	3.531	13.78	16.671
Reflections (<i>I</i> > 2 σ (<i>I</i>))	1842	4095	8549	5325
R (<i>F</i> _o)	0.0258	0.0220	0.0372	0.0282
R _w (<i>F</i> _o)	0.0661	0.0493	0.0839	0.0673
GOF	0.951	1.0249	0.9932	1.0497

Compound	3c	4	5a	5b
Empirical formula	Cd ₂ Ag ₅ P ₂ N ₁₁ C ₄₆ H ₃₀	Cd ₁ Ag ₃ P ₂ N ₇ C ₄₈ H _{48.87} O _{3.44}	Mn ₁ Au ₃ P ₁ N ₆ C ₂₄ H ₁₅	Cd ₁ Au ₃ P ₁ N ₆ C ₂₄ H ₁₅
Formula weight (g mol ^{−1})	1653.04	1276.78	1340.52	1398
Crystal System	Monoclinic	Cubic	Monoclinic	Monoclinic
Space Group	<i>C2/c</i> (No. 15)	<i>Pa</i> $\bar{3}$ (No. 205)	<i>I2/a</i> (No. 15)	<i>I2/a</i> (No. 15)
Z	4	8	4	4
Radiation (Å)	Cu K α , λ = 1.54180	Mo K α , λ = 0.71073	Mo K α , λ = 0.71073	Cu K α , λ = 1.54180
Crystal colour	Colourless	Colourless	Colourless	Colourless
Crystal size (mm)	0.04 × 0.10 × 0.23	0.19 × 0.34 × 0.39	0.06 × 0.08 × 0.10	0.02 × 0.02 × 0.10
Temperature (K)	282(8)	280.0(4)	150.0(5)	291.8(1)
<i>a</i> (Å)	28.5577(8)	21.7394(3)	16.7035(3)	16.8455(3)
<i>b</i> (Å)	15.8350(4)	21.7394(3)	12.5777(3)	12.7383(3)
<i>c</i> (Å)	13.9531(4)	21.7394(3)	20.6707(4)	20.8965(3)
<i>V</i> (Å ³)	6226.6(3)	10274.1(2)	4338.48(15)	4480.19(15)
β (°)	99.310(3)	—	92.5382(10)	92.3725(16)
μ (mm ^{−1})	18.499	1.633	10.509	22.772
Reflections (<i>I</i> > 2 σ (<i>I</i>))	5585	5085	4065	4094
R (<i>F</i> _o)	0.0400	0.0388	0.0377	0.0226
R _w (<i>F</i> _o)	0.1148	0.0820	0.0668	0.0525
GOF	0.958	1.0363	1.067	0.9997

geometry and cyanide binding orientation: the node cations are tetrahedrally coordinated by the N cyanide terminus and the linker cations are linearly coordinated by the C cyanide terminus. The crystal structure is illustrated in Figure 2, and relevant crystallographic details are summarized in Table 2. Three distorted diamondoid networks interpenetrate, with each [NEt₄]⁺ cation contained within a cavity formed by the combination of all three networks.

An intriguing property of this system is the existence of a phase transition on cooling below 235 K. This transition—which will be described in detail elsewhere—involves the condensation of a soft phonon mode at an incommensurate wave-vector. The study of classical soft-mode transitions in extended frameworks is a relatively unexplored field;^{95,96} the purpose of drawing attention to this transition here is simply to highlight that the dynamical properties of these materials may, in due course, be of interest in their own right.

Five-Connected A_{0.5}BX_{2.5}. Reaction of [NBu₄][Ag(CN)]·0.5H₂O with cadmium nitrate leads to the structurally complex phase [NBu₄]_{0.5}Cd^{II}[Ag(CN)₂]_{2.5} (**2**), as illustrated in Figure 2. Key crystallographic details of **2** are again summarized in Table 2. In the absence of a strong coordination preference, Cd^{II} has here adopted a distorted trigonal bipyramidal geometry. These

pentacoordinate nodes connect to give a unique, self-catenating topology (TOPOS reference *jah1*; the topology was detected with TOPOS^{97,98} and deposited in the TTD⁹⁹ archive) that can be related to a linked pair of interpenetrating cds-type nets (see Supporting Information (SI)). Mindful that correlation does not necessarily imply causation, we note nonetheless that there is again a close match between framework cavity and molecular cation shape. This suggests that the form of the [NBu₄]⁺ cation may be responsible for the unusual topology assumed by this material.

As in **1** and numerous other dicyanoargentate frameworks, **2** contains a series of short Ag^I...Ag^I contacts generally considered indicative of d¹⁰...d¹⁰ argentophilic interactions. These interactions are often strongly susceptible to changes in external conditions, such as temperature and pressure.^{100–105} We determined the thermal expansion behavior of **2** in order to identify any unusual thermomechanical response, and found moderately strong positive and negative thermal expansion in directions that are respectively parallel and perpendicular to these argentophilic interactions (α_{\parallel} = +138(5) MK^{−1}, α_{\perp} = −83.1(1.6) MK^{−1}; see SI for further discussion).¹⁰⁶

An alternative five-connected dicyanometallate structure that is more obviously related to the molecular perovskite analogues

discussed above can be accessed by reaction of $[\text{PPN}]^+$ dicyanometallates with transition-metal salts ($[\text{PPN}]^+ = \text{bis}(\text{triphenylphosphine})\text{iminium cation}$). The crystal structures of $[\text{PPN}]_{0.5}\text{Cu}[\text{Au}(\text{CN})_2]_{2.5} \cdot \text{EtOH}$ (**3a**), $[\text{PPN}]_{0.5}\text{Mn}[\text{Ag}(\text{CN})_2]_{2.5}(\text{EtOH})$ (**3b**), and $[\text{PPN}]_{0.5}\text{Cd}[\text{Ag}(\text{CN})_2]_{2.5}(\text{EtOH})$ (**3c**) are shown in Figure 2, and key crystallographic details are again summarized in Table 2. In these compounds, the dicyanometallate network forms grid-like layers of connected cubes that are then stacked on top of one another. The large molecular cations occupy the voids at the center of each $\sim(\text{nm})^3$ cube. Because the layers are not connected, each transition metal node is coordinated by dicyanometallate anions in a square pyramidal geometry. Whereas in the case of Cu^{2+} this coordination geometry is straightforwardly understood in terms of the d^9 electronic configuration, for **3b** and **3c** the Mn^{2+} and Cd^{2+} coordination is actually octahedral and is completed by one molecule of the ethanol solvent from which the crystals were grown. The ability to incorporate octahedral node geometries via solvent coordination means that, in principle at least, this phase may be accessible for a range of other transition-metal dications. In practice, the balance with competing phases (discussed further below) is remarkably subtle.

In each of the compounds **3a–c**, successive layers are offset by one-half of the cube face diagonal. This offset has the effect of bringing Ag^+ or Au^+ cations at the cube edges into close contact, which will presumably maximize metallophilic interactions. In this sense there is a clear distinction from the structural chemistry of oxide frameworks, where there is a strong repulsion between the linker anions. In the related $n = 2$ Ruddlesden–Popper phases (e.g., $\text{Sr}_3\text{Ti}_2\text{O}_7$) this repulsion is relieved by presence of additional A-cations as rocksalt-type layers.¹⁰⁷ In our case, the weak metallophilic forces holding neighboring layers together may be expected to result in particularly anisotropic elastic response for this family,¹⁰⁸ while also allowing for the possibility of intercalation chemistry.^{109–111}

Cubic ABX_3 . The analogy between dicyanometallate frameworks and perovskite oxides is clearest in the last family of compounds we report. These again make use of the $[\text{PPN}]^+$ dicyanometallates in their synthesis. Similar conditions to those described above for **3a–c** allowed preparation of the ABX_3 solvate $[\text{PPN}]\text{Cd}[\text{Ag}(\text{CN})_2]_3 \cdot 3\text{EtOH}$ (**4**) and the solvent-free frameworks $[\text{PPN}]\text{Mn}[\text{Au}(\text{CN})_2]_3$ (**5a**) and $[\text{PPN}]\text{Cd}[\text{Au}(\text{CN})_2]_3$ (**5b**). In the case of **4**, crystals grew directly from reaction mixtures that had originally formed crystals of **3c**; the relationship between these phases is discussed in more detail below. The structures of all three compounds **4**, **5a**, **5b** are clear analogues of perovskites: octahedrally coordinated $\text{Mn}^{\text{II}}/\text{Cd}^{\text{II}}$ centers are connected to form the characteristic cubic network, with $[\text{PPN}]^+$ cations adopting the “12-coordinate” A-cation site [Figure 2]. We use the term “super-perovskites” to reflect this structural correspondence and to emphasize that the B–B separation across the perovskite cube edge is now on the nanometre scale.

Just as for other perovskite analogues, long-established geometric descriptors can be applied to these superperovskite frameworks. For example, we calculate “tolerance factors” of 1.02 (at 150 K) and 1.00 (at 300 K) for **5a** and **5b**, respectively (see SI);^{112–114} likewise the octahedral tilt systems active in both structures correspond to the same Glazer notation $a^-a^-c^-$.^{115,116} While the tilts of compounds **5a** and **5b** can be described completely using Glazer notation, compound **4**

shows in-phase tilting of adjacent octahedra correlated perpendicular to the rotation axis: an impossibility for perovskites, such as oxides and halides, with monatomic anions. The tilt system of **4** is described by the following tilt tensor (see SI for discussion of this notation):

$$\begin{bmatrix} - & - & + \\ + & - & - \\ - & + & - \end{bmatrix}$$

Because the phenyl groups of the PPN^+ cation extend up to the perovskite cube faces, there are direct cation–cation interactions that may influence the phase transition behavior of these systems. In contrast to the simple monopolar and/or dipolar interactions between A-site cations in oxide perovskites, these interactions are inherently multipolar, which in turn may give rise to complex ordering processes unrealisable in conventional ceramics. Indeed the PPN^+ conformations we observe in compound **3c** and its transformation product **4** are fundamentally different from those found in **5a** and **5b**: in the former the phenyl rings are oriented as if to maximize cation– π interactions with the linker Ag^+ cation, whereas in the latter intra- and inter-molecular π – π interactions dominate (Figure 3a,b). This is entirely consistent with the diversity of $\text{PPN}^+ \cdots \text{PPN}^+$ supramolecular interaction motifs known to occur in the solid state.¹¹⁷ So one alternative view of the structures of **5a** and **5b** is that the anionic dicyanometallate framework acts to impose a particular geometric arrangement of the PPN^+ cations that may not necessarily be compatible with the inter-cation interactions. We suggest that exploration of this tension between complex multipolar interactions and the geometry of the lattice supporting those interactions may be a fertile playground for future research given, for example, the implication of multipolar dynamics in extending charge-carrier lifetimes in $[\text{CH}_3\text{NH}_3]\text{PbI}_3$ (Figure 3c,d).¹¹⁸

Composition–Structure Relationships in Dicyanometallates. Given the diversity of known structures of dicyanometallate frameworks—i.e., those reported in the preceding section together with the exhaustive list given in Table 1—it is natural to ask how one might control the adoption of one architecture or another through choice of chemical composition. Our approach to answering this question is essentially an empirical one. We begin by organizing all known dicyanometallates into compositional families of given stoichiometry A_mBX_n . Even if their structures vary, members of any one family share the same coordination number and charge state of the $\text{B}^{(n-m)+}$ cation—two aspects over which the synthetic chemist has some control. Coordination number usually fixes the value of n and so constrains the number and type of relevant network topologies. Likewise, cation charge determines the value of $n - m$ and so determines the extent of inclusion of extra-framework A^+ cations (i.e., the value of m). A visual representation of our categorization is given in Figure 4, and it is by interpreting the various trends that emerge from this diagram that we ultimately aim to devise design strategies linking chemical composition and framework structure.

What is immediately obvious is that some families are considerably more populous than others. The largest and most topologically diverse family is that with composition BX_2 , consisting of a variety of structures based on four-connected nets. Four-fold connectivity is well known¹¹⁹ to favor topological diversity—hence the polymorphism of, e.g., silica, zeolites, and imidazolate MOFs.¹²⁰ In the present case,

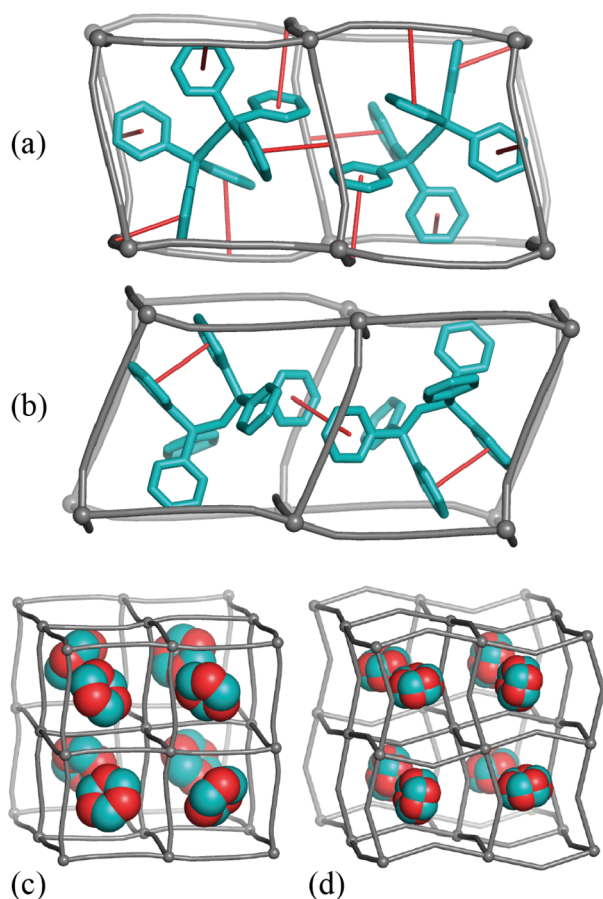
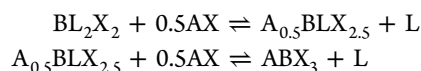


Figure 3. Short cation– π and π – π interactions in **3c** (a) and **5b** (b). Distances shorter than 4.2 Å are indicated by red lines. In **3c** the phenyl rings are oriented such that short cation– π distances are maximized, whereas in **5b** intra- and inter-molecular π – π interactions dominate. Crucially, the latter are present between adjacent [PPN]⁺ cations. [PPN]⁺ cations are inherently multipolar and their packing in **4** (c) corresponds to ordered hexapoles. Such multipolar interactions are common for framework materials with molecular cations such as [CH₃NH₃]₂PbI₃ (d) where the dynamics of these interactions are implicated in slow exciton recombination (cation-ordered *Pnma* structure shown).^{31,118} Framework shown in gray, cation in teal (a,b), and multipoles in teal and red (c,d); H atoms not shown for clarity.

Zn[Au(CN)₂]₂ emerges as the most polymorphic of the BX₂ systems, crystallizing in at least four different forms that include analogues of cristobalite and quartz.¹⁴ In fact the parallel with silica is a meaningful one: the combination of tetrahedral Zn²⁺ coordination geometry and aurophilic interactions capable of bending the Zn–NC–Au–CN–Zn linkers resembles strongly the nonlinear Si–O–Si building units of SiO₂ frameworks. But one additional reason for the accessibility of these BX₂ structures will likely be the large number of divalent cations with aqueous chemistry. Even transition metals with octahedral coordination can yield four-connected frameworks if spectator ligands are present in the synthesis mixture (noting that sometimes solvent itself may play this role). Indeed it is the doubly ligated octahedral [*trans*-BX₄L₂] coordination motif that yields the square grid topology—the most frequently adopted network structure observed for this family.

In principle, any such coordinated ligands may be susceptible to exchange for dicyanometallate anions present in the reaction

mixture, with concomitant incorporation of extra-framework cations:



The equilibrium position will depend on, among other factors, the ligand binding strength and the stoichiometry of AX dicyanometallate salt in the reaction mixture. So, for example, while the Cd²⁺/K[Ag(CN)₂] system forms the B(L₂)X₂ phase Cd(py)₂[Ag(CN)₂]₂ when prepared in the presence of pyridine, in the absence of pyridine the same pair of reagents yields the ABX₃ phase KCd[Ag(CN)₂]₃. Likewise for the Cd²⁺/[PPN][Ag(CN)₂] system we obtain the five-coordinate A_{0.5}B(L)X_{2.5} phase [PPN]_{0.5}Cd(EtOH)[Ag(CN)₂]_{2.5} (**3c**) as a first (kinetic) product; subsequent exposure to additional [PPN][Ag(CN)₂] drives formation of the superperovskite ABX₃ phase [PPN]Cd[Ag(CN)₂]₃·3EtOH·*n*H₂O (**4**).

This strategy of varying B²⁺:AX stoichiometry seems an attractive method of controlling network connectivity throughout the A_xBX_{2+x} families. The particular topology adopted for the *x* ≠ 0 phases then depends on the geometry of the A⁺ cation. For monatomic A⁺ (e.g., K⁺, Na⁺), the topology is usually that of the corresponding A-deficient framework: this is presumably a consequence of the much larger scale of the dicyanometallate linker. So, for example, both KFe[Ag(CN)₂]₃ and Fe[Ag(CN)₂]₃ share the same triply interpenetrating α -Po network structure. Larger, molecular cations force topological changes that reflect the cation shape. On the one hand, the cruciform conformation of [NBu₄]⁺ helps drive the unusual topologies of [NBu₄]_{0.5}Cd[Ag(CN)₂]_{2.5} and [NBu₄]_{0.5}Ni[Au(CN)₂]₃. On the other hand, the more isotropic [PPN]⁺ cation clearly favors the cubic-type nets of [PPN]_{0.5}Cu[Au(CN)₂]_{2.5}·EtOH and [PPN]Mn[Au(CN)₂]₃.

Although there are far fewer examples based on monovalent B⁺ cations—the need for aqueous chemistry limiting these systems to coinage metal salts—precisely these same trends are observed. Again we find that inclusion of monatomic extra-framework cations appears to have essentially no effect on framework topology: KCu^I[Ag(CN)₂]₂ and Cu^{II}(DMF)[Au(CN)₂]₂ share the same basic square-grid structures. The tetrahedral [NEt₄]⁺ cation now favors a diamondoid topology in [NEt₄]_{0.5}Ag[Ag(CN)₂]₂ and in [Cu₂(2,2'-bpy)₂(CN)]_{0.5}Cu[Cu(CN)₂]_{1.5} the linear nature of the [Cu₂(2,2'-bpy)₂(CN)]⁺ cation drives a honeycomb structure with linear channels. Notable by its absence is the (10,3)-*a* or *srs* topology, a common topology for 3-connected MOFs.⁵ The apparent rarity of 3-connected structures is in large part due to the propensity for Cu⁺ to adopt alternative binding modes, such as bifurcated linkages,²⁴ though it may be possible to make a dicyanometallate framework with (10,3)-*a* topology using an octahedrally coordinated metal with meridionally disposed capping ligands.¹²¹

The general reliance on solution-phase synthesis—whether strictly necessary or not—is likely responsible for the relative paucity of structures known to contain B cations in the 3+ oxidation state and the complete absence of higher-valent examples. All known trivalent dicyanometallate salts adopt one of just two dense framework structures: either the triply interpenetrating α -Po net of Fe[Ag(CN)₂]₃ or the triply interpenetrating *acs* net of the lanthanide salts [Ln(OH₂)₃][Au/Ag(CN)₂]₃. The contrast with the structural diversity of divalent BX₂ systems could hardly be clearer, and will reflect

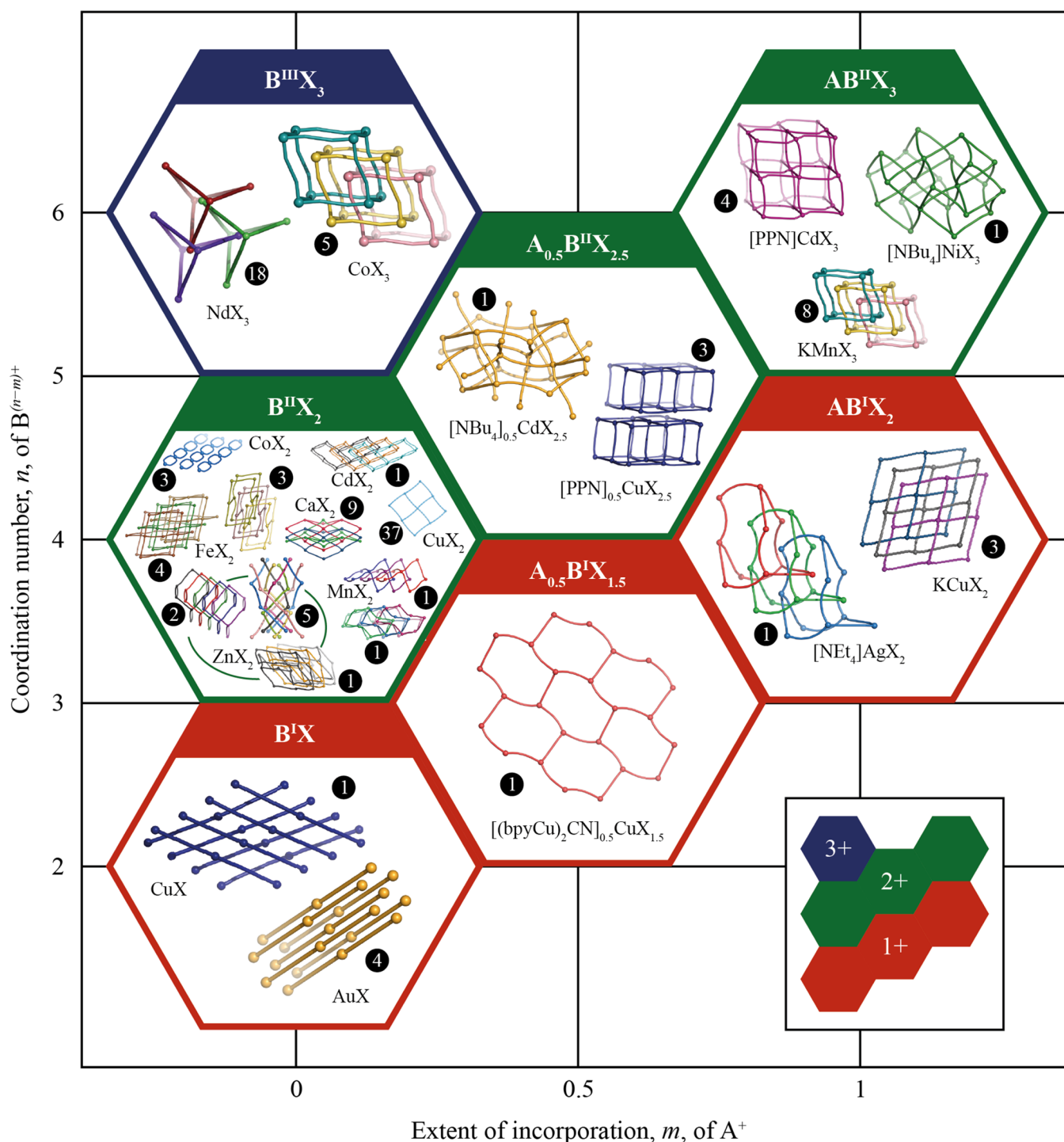


Figure 4. Organization of all known dicyanometallate frameworks according to node coordination number and extent of incorporation of extra-framework cations. The frameworks shown are representative examples of isostructural compounds; the number of such compounds known is given in the corresponding black circle. The collection of frameworks contained within a single hexagonal cell form a family with related composition $A_m B X_n$. The color of the cell corresponds to the charge on the nodal cation (inset).

also the disparity of topological constraints associated with six- and four-connected nodes. In principle, it may be possible to access more open structure types through incorporation of extra-framework cations. Naturally, this would require coordination numbers higher than six—which is certainly feasible for the lanthanide trications. Consequently, further exploration¹²² of lanthanide dicyanometallate chemistry using *molecular AX*

sources may yield as-yet unrealised systems with compositions $A_{0.5}B X_{3.5}$ and/or ABX_4 .

In addition to the general trends we discuss here, a number of interesting comparisons can be drawn between neighboring pairs of structural families as shown in Figure 4. For example, there are clear diagonal relationships which connect the topologies of higher- and lower-connected network structures. In this way, the Ruddlesden–Popper-like structure of

[PPN]_{0.5}Cu[Au(CN)₂]_{2.5}·EtOH (an A_{0.5}BX_{2.5} framework) can be seen as a natural extension of the square-grid structures of both Cu[Ag(CN)₂]₂ and KCu[Ag(CN)₂]₂ (BX₂ and ABX₂ frameworks, respectively). And then the superperovskite [PPN]Cd[Au(CN)₂]₃ structure emerges as a further extension on this same theme. The triad of BX/A_{0.5}BX_{1.5}/ABX₂ systems Cu[Cu(CN)₂]/[Cu₂(2,2'-bpy)₂(CN)]_{0.5}Cu[Cu(CN)₂]_{1.5}/KCu[Cu(CN)₂]₂ can be viewed in precisely the same terms. We anticipate there are many more such relationships, some of which may become increasingly apparent only as new dicyanometallate frameworks continue to be discovered.

CONCLUSIONS

While it has long been clear that a large variety of dicyanometallate frameworks can be prepared, what we have shown here is how the structures of these frameworks might be influenced rationally through variation in cation charge, coordination number, presence of coordinating ligands, and extra-framework cation size, shape and extent of incorporation. The ability to controllably explore a variety of network structures in this way reflects Robson's original vision for coordination polymer chemistry, and suggests that dicyanometallates might be considered a model family for extended framework design. In principle the diversity of structures accessible to this family also suggests a similar diversity of physical properties. Moreover, the structural flexibility imparted by the dicyanometallate linker means that these properties may be much more extreme in nature than in conventional ceramic frameworks—as is already known to be the case in a number of examples.^{12,13}

But what we see as particularly attractive about dicyanometallate framework chemistry is the ability to include complex molecular cations within a number of different framework topologies. So much of the rich structural chemistry and physics of conventional ceramic frameworks has arisen from the interplay between lattice geometry, local degrees of freedom, and nature of intersite interactions. Consequently the extension of these same concepts to systems with *new* degrees of freedom (e.g., molecular cation orientations and conformations), *new* lattice geometries (e.g., the topology of compound 2), and *new* types of interactions (e.g., cation- π and π - π) augurs well for the discovery of new and interesting physical phenomena in this intriguing model family of framework structures.

METHODS

Sample Preparation. Dicyanometallate Precursors. [NBu₄]Ag(CN)₂·0.5H₂O was prepared by adding an aqueous solution of [NBu₄]CN (0.5510 g in 400 mL water) to a suspension of AgCN (0.3435 g in 100 mL water) and stirring for 1 h. The excess AgCN was then removed by vacuum filtration and the volume of the filtrate reduced by rotary evaporation. The concentrated filtrate was allowed to evaporate, and the resulting powder was dried at 50 °C for 2.5 h and then at 40 °C for 18 h.

[PPN]Au(CN)₂ was prepared by the method outlined in ref 32. Solutions of KAu(CN)₂ (2.583 g in 100 mL water) and PPNCl (5.40 g in 200 mL 50:50 water:ethanol) were combined with immediate formation of a white precipitate. The reaction mixture was covered and stirred for 1 h then collected by vacuum filtration and washed with 300 mL cold water. The solid was left to air-dry overnight then dried in a vacuum oven at 40 °C for 3.5 h giving 6.80 g of product (Yield: 96.3%). Elemental analysis: Found (calculated)% C 57.74 (57.95); H 3.80 (3.84); N 5.24 (5.34).

[PPN]Ag(CN)₂ was prepared by a similar method to [PPN]Au(CN)₂. Solutions of KAg(CN)₂ (1.881 g in 100 mL water) and PPNCl

(5.68 g in 200 mL 50:50 water:ethanol) were combined with immediate formation of a white precipitate. The reaction mixture was covered and stirred for 1 h then collected by vacuum filtration and washed with 300 mL cold water. The solid was left to air-dry overnight then dried in a vacuum oven at 40 °C for 1 week giving 5.87 g of product (Yield: 90.0%). Elemental analysis: Found (calculated)% C 65.05 (65.34); H 4.26 (4.33); N 5.88 (6.02).

Dicyanometallate Frameworks. [NEt₄]Ag[Ag(CN)₂]₂ (1) single crystals were prepared by slow evaporation of aqueous solutions of KAg(CN)₂ and [NEt₄]Cl. Solutions of KAg(CN)₂ (0.2802 g, 1.411 mmol) and [N(C₂H₅)₄]Cl (0.2380 g, 1.436 mmol) were prepared with the minimum quantity of water and then mixed. The resulting colorless solution was left to evaporate slowly and crystals formed within 3 weeks.

[NBu₄]_{0.5}Cd[Ag(CN)₂]_{2.5} (2) Aqueous solutions of [NBu₄]Ag(CN)₂·0.5H₂O and Cd(NO₃)₂·4H₂O were prepared with the minimum quantity of solvent, mixed, and left to evaporate from an open Petri dish. Crystals were harvested after a few days.

[PPN]_{0.5}Cu[Au(CN)₂]_{2.5}·EtOH (3a) single crystals were prepared by slow-diffusion in an H-cell. Into one arm was placed [PPN]Au(CN)₂ (25 mg in 1 mL of ethanol) and the other CuCl₂·2H₂O (5.4 mg in 0.142 mL of ethanol). The remaining volume was carefully made up with cold ethanol. Green crystals grew in the [PPN]Au(CN)₂ arm after 2 days.

[PPN]_{0.5}Mn[Ag(CN)₂]_{2.5}(EtOH) (3b) was prepared by diffusion in a Schott bottle. Cold solutions of [PPN]Ag(CN)₂ (1.125 g in 20 mL of ethanol) and Mn(NO₃)₂·4H₂O (148 mg in 6 mL of ethanol) were carefully layered with a buffer of 50 mL cold ethanol separating the layers. Crystals formed overnight.

[PPN]_{0.5}Cd[Ag(CN)₂]_{2.5}·EtOH (3c) single crystals were prepared by slow-diffusion in a vial. Cold solutions of [PPN]Ag(CN)₂ (101 mg in 2 mL of ethanol) and Cd(NO₃)₂·4H₂O (19 mg in 0.2 mL of ethanol) were carefully layered with a buffer of 5 mL of cold ethanol separating the layers. Crystals formed overnight.

For [PPN]Cd[Ag(CN)₂]₃·3EtOH·*n*H₂O (4), a crystal was selected from a small portion (roughly 3 mL) of a reaction mixture that initially yielded 3c. Solutions of [PPN]Ag(CN)₂ (1.108 g in 25 mL of ethanol) and Cd(NO₃)₂·4H₂O (183.7 mg in 7 mL of ethanol) with a buffer of 50 mL of ethanol separating the layers in a Schott bottle. Colorless crystals formed overnight and then a portion of these crystals, with mother liquor, were set aside in a sealed sample tube. After 10 weeks a crystal of compound 4 was selected from this portion.

[PPN]Mn[Au(CN)₂]₃ (5a) was prepared by layering ethanolic solutions of PPNAu(CN)₂ (50 mg in 2 mL of ethanol) and Mn(CIO₄)₂·xH₂O (14 mg in 0.2 mL of ethanol) in a small sample tube. Colorless crystals formed after 1 h.

[PPN]Cd[Au(CN)₂]₃ (5b) was prepared by layering ethanolic solutions of PPNAu(CN)₂ (50 mg in 2 mL of ethanol) and Cd(NO₃)₂·4H₂O (21 mg in 0.2 mL of ethanol) in a small sample tube. Colorless crystals formed after 1 h.

Single-Crystal X-ray Diffraction. Single-crystal X-ray diffraction data were collected using a Nonius KappaCCD diffractometer (2 and 5a) or an Oxford Diffraction (Rigaku Oxford Diffraction) SuperNova diffractometer (1, 3b, 3c, 4, 5b) fitted with an Oxford Cryosystems Cryostream 600 Series/700 Plus open-flow nitrogen cooling device.¹²³ Data for 3a were collected at Diamond Light Source (beamline I19)¹²⁴ fitted with an Oxford Cryosystems HeliX open-flow helium cryostat.¹²⁵ DENZO/SCALEPACK,¹²⁶ CrysAlisPro,¹²⁷ or CrystalClear were used for data collection and reduction as appropriate. The structures were solved *ab initio* using SIR92¹²⁸ or SUPERFLIP.¹²⁹ All structures were refined with full-matrix least-squares on *F*² using CRYSTALS.^{130,131} Hydrogen atoms were, in some cases, visible in the difference Fourier map and treated in the usual manner.¹³² In the remaining cases, and particularly for disordered assemblies, hydrogen atoms were added geometrically. Full structural data are included in the SI, including CIF files, and have been submitted to the CCDC as numbers 1444134–1444141. These data can also be obtained free of charge from The Cambridge Crystallographic Data Centre via http://www.ccdc.cam.ac.uk/data_request/cif.

■ ASSOCIATED CONTENT

■ Supporting Information

The Supporting Information is available free of charge on the ACS Publications website at DOI: 10.1021/jacs.5b13446.

X-ray crystallographic data for **1**, **2**, **3a**, **3b**, **3c**, **4**, **5a**, **5b**, **S1**, and **S2** (CIF)

Single-crystal X-ray structural information and methods for [PPN]Au/Ag(CN)₂, variable-temperature single-crystal X-ray diffraction studies, powder diffraction data, TGA data, tolerance factor calculations, and topology decomposition of **2** (PDF)

■ AUTHOR INFORMATION

Corresponding Author

*andrew.goodwin@chem.ox.ac.uk

Notes

The authors declare no competing financial interest.

■ ACKNOWLEDGMENTS

The authors gratefully acknowledge financial support from the ERC (Grant 279705) and the EPSRC (Grant EP/G004528/2). We are extremely grateful for the award of beamtime to the Block Allocation Group (MT9981) used to collect the single crystal synchrotron X-ray diffraction data on the I19 beamline at the Diamond Light Source. J.A.H. thanks G. Kieslich for helpful conversations regarding tolerance factors and V. A. Blatov for comments on the topology of compound **2**.

■ REFERENCES

- (1) Hoskins, B. F.; Robson, R. *J. Am. Chem. Soc.* **1990**, *112*, 1546–1554.
- (2) Yaghi, O. M.; O’Keeffe, M.; Ockwig, N. W.; Chae, H. K.; Eddaoudi, M.; Kim, J. *Nature* **2003**, *423*, 705–714.
- (3) Côté, A. P.; El-Kaderi, H. M.; Furukawa, H.; Hunt, J. R.; Yaghi, O. M. *J. Am. Chem. Soc.* **2007**, *129*, 12914–12915.
- (4) Feng, X.; Ding, X.; Jiang, D. *Chem. Soc. Rev.* **2012**, *41*, 6010–6022.
- (5) Ockwig, N. W.; Delgado-Friedrichs, O.; O’Keeffe, M.; Yaghi, O. M. *Acc. Chem. Res.* **2005**, *38*, 176–182.
- (6) Eddaoudi, M.; Kim, J.; Vodak, D.; Sudik, A.; Wachter, J.; O’Keeffe, M.; Yaghi, O. M. *Proc. Natl. Acad. Sci. USA* **2002**, *99*, 4900–4904.
- (7) Sonnauer, A.; Hoffmann, F.; Fröba, M.; Kienle, L.; Duppel, V.; Thommes, M.; Serre, C.; Férey, G.; Stock, N. *Angew. Chem., Int. Ed.* **2009**, *48*, 3791–3794.
- (8) Deng, H.; Grunder, S.; Cordova, K. E.; Valente, C.; Furukawa, H.; Hmadeh, M.; Gándara, F.; Whalley, A. C.; Liu, Z.; Asahina, S.; Kazumori, H.; O’Keeffe, M.; Terasaki, O.; Stoddart, J. F.; Yaghi, O. M. *Science* **2012**, *336*, 1018–1023.
- (9) Farha, O. K.; Malliakas, C. D.; Kanatzidis, M. G.; Hupp, J. T. *J. Am. Chem. Soc.* **2010**, *132*, 950–952.
- (10) Loiseau, T.; Serre, C.; Huguenard, C.; Fink, G.; Taulelle, F.; Henry, M.; Bataille, T.; Férey, G. *Chem.–Eur. J.* **2004**, *10*, 1373–1382.
- (11) Volklinger, C.; Loiseau, T.; Devic, T.; Férey, G.; Popov, D.; Burghammer, M.; Riekel, C. *CrystEngComm* **2010**, *12*, 3225–3228.
- (12) Goodwin, A. L.; Calleja, M.; Conterio, M. J.; Dove, M. T.; Evans, J. S. O.; Keen, D. A.; Peters, L.; Tucker, M. G. *Science* **2008**, *319*, 794–797.
- (13) Cairns, A. B.; Catafesta, J.; Levelut, C.; Rouquette, J.; van der Lee, A.; Peters, L.; Thompson, A. L.; Dmitriev, V.; Haines, J.; Goodwin, A. L. *Nat. Mater.* **2013**, *12*, 212–216.
- (14) Katz, M. J.; Ramnial, T.; Yu, H.-Z.; Leznoff, D. B. *J. Am. Chem. Soc.* **2008**, *130*, 10662–10673.
- (15) Abrahams, S. C.; Bernstein, J. L.; Liminga, R.; Eisenmann, E. T. *J. Chem. Phys.* **1980**, *73*, 4585–4590.
- (16) Colis, J. C. F.; Larochelle, C.; Fernández, E. J.; López-de Luzuriaga, J. M.; Monge, M.; Laguna, A.; Tripp, C.; Patterson, H. J. *Phys. Chem. B* **2005**, *109*, 4317–4323.
- (17) Lefebvre, J.; Batchelor, R. J.; Leznoff, D. B. *J. Am. Chem. Soc.* **2004**, *126*, 16117–16125.
- (18) Niel, V.; Muñoz, M. C.; Gaspar, A. B.; Galet, A.; Levchenko, G.; Real, J. A. *Chem.–Eur. J.* **2002**, *8*, 2446–2453.
- (19) Hill, J. A.; Cairns, A. B.; Lim, J. J. K.; Cassidy, S. J.; Clarke, S. J.; Goodwin, A. L. *CrystEngComm* **2015**, *17*, 2925–2928.
- (20) Rao, C. N. R. *Annu. Rev. Phys. Chem.* **1989**, *40*, 291–326.
- (21) Cox, P. A. *Transition Metal Oxides: An Introduction to Their Electronic Structure and Properties*; Clarendon Press: Oxford, UK, 2010.
- (22) Sharpe, A. G. *The Chemistry of Cyano Complexes of the Transition Metals*; Academic Press: London, 1976.
- (23) Dunbar, K. R.; Heintz, R. A. *Progress in Inorganic Chemistry*; John Wiley & Sons, Inc.: Hoboken, NJ, USA, 2007; pp 283–391.
- (24) Alexandrov, E. V.; Virovets, A. V.; Blatov, V. A.; Peresypkina, E. V. *Chem. Rev.* **2015**, *115*, 12286–12319.
- (25) Wang, Z.; Zhang, B.; Otsuka, T.; Inoue, K.; Kobayashi, H.; Kurmoo, M. *Dalton Trans.* **2004**, 2209–2216.
- (26) Hu, K.-L.; Kurmoo, M.; Wang, Z.; Gao, S. *Chem.–Eur. J.* **2009**, *15*, 12050–12064.
- (27) Collings, I. E.; Hill, J. A.; Cairns, A. B.; Cooper, R. I.; Thompson, A. L.; Parker, J. E.; Tang, C. C.; Goodwin, A. L. *Dalton Trans.* **2016**, *45*, 4169–4178.
- (28) Lee, M. M.; Teuscher, J.; Miyasaka, T.; Murakami, T. N.; Snaith, H. J. *Science* **2012**, *338*, 643–647.
- (29) Stoumpos, C. C.; Malliakas, C. D.; Kanatzidis, M. G. *Inorg. Chem.* **2013**, *52*, 9019–9038.
- (30) Motta, C.; El-Mellouhi, F.; Kais, S.; Tabet, N.; Alharbi, F.; Sanvito, S. *Nat. Commun.* **2015**, *6*, 7026.
- (31) Weller, M. T.; Weber, O. J.; Henry, P. F.; Di Pumpo, A. M.; Hansen, T. C. *Chem. Commun.* **2015**, *51*, 4180–4183.
- (32) Lefebvre, J.; Chartrand, D.; Leznoff, D. B. *Polyhedron* **2007**, *26*, 2189–2199.
- (33) Eisenmann, E. T. *J. Electrochem. Soc.* **1977**, *124*, 1957–1958.
- (34) Zhdanov, G. S.; Shugam, E. A. *Acta Physicochimica U.R.S.S.* **1945**, *20*, 253.
- (35) Bowmaker, G. A.; Kennedy, B. J.; Reid, J. C. *Inorg. Chem.* **1998**, *37*, 3968–3974.
- (36) Lefebvre, J.; Korčok, J. L.; Katz, M. J.; Leznoff, D. B. *Sensors* **2012**, *12*, 3669–3692.
- (37) Soma, T.; Iwamoto, T. *Chem. Lett.* **1995**, *24*, 271–272.
- (38) Hoskins, B. F.; Robson, R.; Scarlett, N. V. Y. *J. Chem. Soc., Chem. Commun.* **1994**, 1994, 2025–2026.
- (39) West, C. D. Z. *Kristallogr. Krist.* **1934**, *88*, 173–175.
- (40) West, C. D. Z. *Kristallogr. Krist.* **1935**, *90*, 555–558.
- (41) Yoshida, K.; Kosone, T.; Kanadani, C.; Saito, T.; Kitazawa, T. *Polyhedron* **2011**, *30*, 3062–3066.
- (42) Vlček, A.; Orendáč, M.; Orendáčová, A.; Kajňáková, M.; Papageorgiou, T.; Chomič, J.; Černák, J.; Massa, W.; Feher, A. *Solid State Sci.* **2007**, *9*, 116–125.
- (43) Lefebvre, J.; Trudel, S.; Hill, R. H.; Leznoff, D. B. *Chem. - Eur. J.* **2008**, *14*, 7156–7167.
- (44) Hibble, S. J.; Cheyne, S. M.; Hannon, A. C.; Eversfield, S. G. *Inorg. Chem.* **2002**, *41*, 4990–4992.
- (45) Galet, A.; Muñoz, M. C.; Martínez, V.; Real, J. A. *Chem. Commun.* **2004**, 2268–2269.
- (46) Geiser, U.; Schlueter, J. A. *Acta Crystallogr., Sect. C: Cryst. Struct. Commun.* **2003**, *59*, i21–i23.
- (47) Chakraborty, J.; Nandi, M.; Mayer-Figge, H.; Sheldrick, W. S.; Sorace, L.; Bhaumik, A.; Banerjee, P. *Eur. J. Inorg. Chem.* **2007**, *2007*, 5033–5044.
- (48) Agustí, G.; Gaspar, A. B.; Muñoz, M. C.; Lacroix, P. G.; Real, J. A. *Aust. J. Chem.* **2009**, *62*, 1155–1165.
- (49) Soma, T.; Iwamoto, T. *J. Inclusion Phenom. Mol. Recognit. Chem.* **1996**, *26*, 161–173.
- (50) Korčok, J. L.; Katz, M. J.; Leznoff, D. B. *J. Am. Chem. Soc.* **2009**, *131*, 4866–4871.

- (51) Dong, W.; Zhu, L.-N.; Sun, Y.-Q.; Liang, M.; Liu, Z.-Q.; Liao, D.-Z.; Jiang, Z.-H.; Yan, S.-P.; Cheng, P. *Chem. Commun.* **2003**, 2544–2545.
- (52) Rodríguez-Velamazán, J. A.; Castro, M.; Palacios, E.; Burriel, R.; Kitazawa, T.; Kawasaki, T. *J. Phys. Chem. B* **2007**, *111*, 1256–1261.
- (53) Kosone, T.; Suzuki, Y.; Kanadani, C.; Saito, T.; Kitazawa, T. *Bull. Chem. Soc. Jpn.* **2009**, *82*, 347–351.
- (54) Range, K.-J.; Zabel, M.; Meyer, H.; Fischer, H. *Z. Naturforsch. B* **1985**, *40*, 1618–1621.
- (55) Chesnut, D. J.; Zubieta, J. *Chem. Commun.* **1998**, 1707–1708.
- (56) Wang, S.-P.; Chen, J.; Gao, D.-Z.; Song, Y.; Wang, Q.-M.; Liao, D.-Z.; Jiang, Z.-H.; Yan, S.-P. *J. Coord. Chem.* **2005**, *58*, 1695–1702.
- (57) Katz, M. J.; Michaelis, V. K.; Aguiar, P. M.; Yson, R.; Lu, H.; Kaluarachchi, H.; Batchelor, R. J.; Schreckenbach, G.; Kroeker, S.; Patterson, H. H.; Leznoff, D. B. *Inorg. Chem.* **2008**, *47*, 6353–6363.
- (58) Soma, T.; Iwamoto, T. *Chem. Lett.* **1994**, *23*, 821–824.
- (59) Othong, J.; Wannarit, N.; Pakawatchai, C.; Youngme, S. *Acta Crystallogr., Sect. E: Struct. Rep. Online* **2014**, *70*, 107–110.
- (60) Chippindale, A. M.; Cheyne, S. M.; Hibble, S. J. *Angew. Chem., Int. Ed.* **2005**, *44*, 7942–7946.
- (61) Colacio, E.; Lloret, F.; Kivekäs, R.; Ruiz, J.; Suárez-Varela, J.; Sundberg, M. R. *Chem. Commun.* **2002**, 592–593.
- (62) Kosone, T.; Kanadani, C.; Saito, T.; Kitazawa, T. *Polyhedron* **2009**, *28*, 1930–1934.
- (63) Korkmaz, N.; Karadağ, A.; Aydın, A.; Yanar, Y.; Karaman, I.; Tekin, Ş. *New J. Chem.* **2014**, *38*, 4760–4773.
- (64) Wang, S.-P.; Gao, D.-Z.; Song, Y.; Liu, Z.-Q.; Liao, D.-Z.; Jiang, Z.-H.; Yan, S.-P. *Inorg. Chim. Acta* **2006**, *359*, 505–510.
- (65) Kosone, T.; Tomori, I.; Kanadani, C.; Saito, T.; Mochida, T.; Kitazawa, T. *Dalton Trans.* **2010**, *39*, 1719–1721.
- (66) Muñoz, M. C.; Gaspar, A. B.; Galet, A.; Real, J. A. *Inorg. Chem.* **2007**, *46*, 8182–8192.
- (67) Agustí, G.; Muñoz, M. C.; Gaspar, A. B.; Real, J. A. *Inorg. Chem.* **2008**, *47*, 2552–2561.
- (68) Ludi, A.; Güdel, H. U.; Dvořák, V. *Helv. Chim. Acta* **1967**, *50*, 2035–2039.
- (69) Schröder, U.; Scholz, F. *Inorg. Chem.* **2000**, *39*, 1006–1015.
- (70) Hoskins, B. F.; Robson, R.; Scarlett, N. V. Y. *Angew. Chem., Int. Ed. Engl.* **1995**, *34*, 1203–1204.
- (71) Kawasaki, T.; Kachi-Terajima, C.; Saito, T.; Kitazawa, T. *Bull. Chem. Soc. Jpn.* **2008**, *81*, 268–273.
- (72) Abrahams, S. C.; Zyontz, L. E.; Bernstein, J. L. *J. Chem. Phys.* **1982**, *76*, 5458–5462.
- (73) Goodwin, A. L.; Kennedy, B. J.; Kepert, C. J. *J. Am. Chem. Soc.* **2009**, *131*, 6334–6335.
- (74) Kitazawa, T.; Hiruma, K.; Sato, H.; Tamura, K.; Yamagishi, A. *Dalton Trans.* **2013**, *42*, 16680–16682.
- (75) Guo, Y.; Liu, Z.-Q.; Zhao, B.; Feng, Y.-H.; Xu, G.-F.; Yan, S.-P.; Cheng, P.; Wang, Q.-L.; Liao, D.-Z. *CrystEngComm* **2009**, *11*, 61–66.
- (76) Wannarit, N.; Hahnvanawong, V.; Pakawatchai, C.; Youngme, S. *Transition Met. Chem.* **2012**, *37*, 79–84.
- (77) Colis, J. C. F.; Laroche, C.; Staples, R.; Herbst-Irmer, R.; Patterson, H. *Dalton Trans.* **2005**, 675–679.
- (78) Theppitak, C.; Chainok, K. *Acta Crystallogr. E: Crystallogr. Commun.* **2015**, *71*, m179–m180.
- (79) Ovens, J. S.; Leznoff, D. B. *Dalton Trans.* **2011**, *40*, 4140–4146.
- (80) Assefa, Z.; Haire, R. G.; Sykora, R. E. *J. Solid State Chem.* **2008**, *181*, 382–391.
- (81) Galet, A.; Niel, V.; Muñoz, M. C.; Real, J. A. *J. Am. Chem. Soc.* **2003**, *125*, 14224–14225.
- (82) Soma, T.; Yuge, H.; Iwamoto, T. *Angew. Chem., Int. Ed. Engl.* **1994**, *33*, 1665–1666.
- (83) Assefa, Z.; Kalachnikova, K.; Haire, R. G.; Sykora, R. E. *J. Solid State Chem.* **2007**, *180*, 3121–3129.
- (84) Arcís-Castillo, Z.; Muñoz, M. C.; Molnár, G.; Bousseksou, A.; Real, J. A. *Chem. - Eur. J.* **2013**, *19*, 6851–6861.
- (85) Yoshida, K.; Akahoshi, D.; Kawasaki, T.; Saito, T.; Kitazawa, T. *Polyhedron* **2013**, *66*, 252–256.
- (86) Stier, A.; Range, K.-J. *Z. Kristallogr.* **1997**, *212*, 51–51.
- (87) Yeung, W.-F.; Wong, W.-T.; Zuo, J.-L.; Lau, T.-C. *J. Chem. Soc., Dalton Trans.* **2000**, 629–631.
- (88) Assefa, Z.; Staples, R.; Fackler, J. P., Jr. *Acta Crystallogr., Sect. C: Cryst. Struct. Commun.* **1995**, *51*, 2527–2529.
- (89) Ahern, J. C.; Roberts, R. J.; Follansbee, P.; McLaughlin, J.; Leznoff, D. B.; Patterson, H. H. *Inorg. Chem.* **2014**, *53*, 7571–7579.
- (90) Li, J.-Y.; Ni, Z.-P.; Yan, Z.; Zhang, Z.-M.; Chen, Y.-C.; Liu, W.; Tong, M.-L. *CrystEngComm* **2014**, *16*, 6444–6449.
- (91) Stier, A.; Range, K.-J. *Z. Naturforsch., B: J. Chem. Sci.* **1996**, *51*, 698–702.
- (92) Tanner, P. A.; Zhou, X.; Wong, W.-T.; Kratzer, C.; Yersin, H. *J. Phys. Chem. B* **2005**, *109*, 13083–13090.
- (93) Kalachnikova, K.; Assefa, Z.; Sykora, R. E. *Acta Crystallogr., Sect. E: Struct. Rep. Online* **2007**, *63*, i162.
- (94) Niel, V.; Thompson, A. L.; Muñoz, M. C.; Galet, A.; Goeta, A. E.; Real, J. A. *Angew. Chem., Int. Ed.* **2003**, *42*, 3760–3763.
- (95) Collings, I. E.; Cairns, A. B.; Thompson, A. L.; Parker, J. E.; Tang, C. C.; Tucker, M. G.; Catafesta, J.; Levelut, C.; Haines, J.; Dmitriev, V.; Pattison, P.; Goodwin, A. L. *J. Am. Chem. Soc.* **2013**, *135*, 7610–7620.
- (96) Ryder, M. R.; Civalieri, B.; Bennett, T. D.; Henke, S.; Rudić, S.; Cinque, G.; Fernandez-Alonso, F.; Tan, J.-C. *Phys. Rev. Lett.* **2014**, *113*, 215502.
- (97) Blatov, V. A. *Struct. Chem.* **2012**, *23*, 955–963.
- (98) Blatov, V. A.; Shevchenko, A. P.; Proserpio, D. M. *Cryst. Growth Des.* **2014**, *14*, 3576–3586.
- (99) Alexandrov, E. V.; Blatov, V. A.; Kochetkov, A. V.; Proserpio, D. M. *CrystEngComm* **2011**, *13*, 3947–3958.
- (100) Pyykkö, P. *Chem. Rev.* **1997**, *97*, 597–636.
- (101) Omary, M. A.; Webb, T. R.; Assefa, Z.; Shankle, G. E.; Patterson, H. H. *Inorg. Chem.* **1998**, *37*, 1380–1386.
- (102) Goodwin, A. L.; Keen, D. A.; Tucker, M. G. *Proc. Natl. Acad. Sci. USA* **2008**, *105*, 18708–18713.
- (103) Goodwin, A. L.; Keen, D. A.; Tucker, M. G.; Dove, M. T.; Peters, L.; Evans, J. S. O. *J. Am. Chem. Soc.* **2008**, *130*, 9660–9661.
- (104) Schmidbaur, H.; Schier, A. *Angew. Chem., Int. Ed.* **2015**, *54*, 746–784.
- (105) Jansen, M. *Angew. Chem., Int. Ed. Engl.* **1987**, *26*, 1098–1110.
- (106) Cliffe, M. J.; Goodwin, A. L. *J. Appl. Crystallogr.* **2012**, *45*, 1321–1329.
- (107) Ruddlesden, S. N.; Popper, P. *Acta Crystallogr.* **1958**, *11*, 54–55.
- (108) Ortiz, A. U.; Boutin, A.; Fuchs, A. H.; Coudert, F.-X. *Phys. Rev. Lett.* **2012**, *109*, 195502.
- (109) Hofmann, K. A.; Küspert, F. Z. *Anorg. Allg. Chem.* **1897**, *15*, 204–207.
- (110) Powell, H. M.; Rayner, J. H. *Nature* **1949**, *163*, 566–567.
- (111) Walker, G. F.; Hawthorne, D. G. *Trans. Faraday Soc.* **1967**, *63*, 166–174.
- (112) Goldschmidt, V. M. *Naturwissenschaften* **1926**, *14*, 477–485.
- (113) Kieslich, G.; Sun, S.; Cheetham, A. K. *Chem. Sci.* **2014**, *5*, 4712–4715.
- (114) Kieslich, G.; Sun, S.; Cheetham, A. K. *Chem. Sci.* **2015**, *6*, 3430–3433.
- (115) Glazer, A. M. *Acta Crystallogr., Sect. B: Struct. Crystallogr. Cryst. Chem.* **1972**, *28*, 3384–3392.
- (116) Bovill, S. M.; Saines, P. J. *CrystEngComm* **2015**, *17*, 8319–8326.
- (117) Lewis, G. R.; Dance, I. J. *J. Chem. Soc., Dalton Trans.* **2000**, 299–306.
- (118) Leguy, A. M. A.; Frost, J. M.; McMahon, A. P.; Sakai, V. G.; Kochelmann, W.; Law, C.; Li, X.; Foglia, F.; Walsh, A.; O'Regan, B. C.; Nelson, J.; Cabral, J. T.; Barnes, P. R. F. *Nat. Commun.* **2015**, *6*, 7124.
- (119) Wells, A. F. *Structural Inorganic Chemistry*, 5th ed.; Clarendon Press: Oxford, UK, 1984.
- (120) Banerjee, R.; Phan, A.; Wang, B.; Knobler, C.; Furukawa, H.; O'Keeffe, M.; Yaghi, O. M. *Science* **2008**, *319*, 939–943.
- (121) Kostakis, G. E.; Powell, A. K. *Dalton Trans.* **2010**, *39*, 2449–2450.

- (122) Roberts, R. J.; Li, X.; Lacey, T. F.; Pan, Z.; Patterson, H. H.; Leznoff, D. B. *Dalton Trans.* **2012**, 41, 6992–6997.
- (123) Glazer, J.; Cosier, A. M. *J. Appl. Crystallogr.* **1986**, 19, 105–107.
- (124) Nowell, H.; Barnett, S. A.; Christensen, K. E.; Teat, S. J.; Allan, D. R. *J. Synchrotron Radiat.* **2012**, 19, 435–441.
- (125) Goeta, A. E.; Thompson, L. K.; Sheppard, C. L.; Tandon, S. S.; Lehmann, C. W.; Cosier, J.; Webster, C.; Howard, J. A. K. *Acta Crystallogr., Sect. C: Cryst. Struct. Commun.* **1999**, 55, 1243–1246.
- (126) Otwinowski, Z.; Minor, W. *Methods Enzymol.* **1997**, 276, 307–326.
- (127) *Crysalis PRO*; Agilent Technologies: Yarnton, England, 2010.
- (128) Altomare, A.; Cascarano, G.; Giacovazzo, C.; Guagliardi, A.; Burla, M. C.; Polidori, G.; Camalli, M. *J. Appl. Crystallogr.* **1994**, 27, 435.
- (129) Palatinus, L.; Chapuis, G. *J. Appl. Crystallogr.* **2007**, 40, 786–790.
- (130) Betteridge, P. W.; Carruthers, J. R.; Cooper, R. I.; Prout, K.; Watkin, D. J. *J. Appl. Crystallogr.* **2003**, 36, 1487.
- (131) Parois, P.; Cooper, R. I.; Thompson, A. L. *Chem. Cent. J.* **2015**, 9, 30.
- (132) Cooper, R. I.; Thompson, A. L.; Watkin, D. J. *J. Appl. Crystallogr.* **2010**, 43, 1100–1107.